Journal of Thermal Stresses, 23:95–110, 2000

0149-5739 /00 $12.00 + .00

THREE-DIMENSIONAL ASYMPTOTIC SCHEME FOR PIEZOTHERMOELASTIC LAMINATES

Zhen-Qiang Cheng
Department of Modern Mechanics
University of Science and Technology of China
Anhui, People's Republic of China

R. C. Batra
Department of Engineering Science and Mechanics
Virginia Polytechnic Institute and State University
Blacksburg, Virginia, USA

A three-dimensional asymptotic scheme that combines the transfer matrix method and the asymptotic expansion technique is used to analyze thermo-electro-mechanical deformations of a piezothermoelastic laminate with surface tractions, electric potentials, and temperatures specified on its top and bottom surfaces. The scheme results in a hierarchy of two-dimensional equations with the same homogeneous operator for each order. For an elastic problem, the homogeneous operator reduces to that for classical thin-plate equations. Results computed for a simply supported rectangular plate with edges grounded are found to be in excellent agreement with the exact solution of the problem.

Piezoelectric materials are often used as sensors and actuators for active control of structural systems [1–7]. Several investigations [8–18] have been carried out to analyze the effects of temperature changes in piezothermoelastic materials. In particular, Xu et al. [16, 17] have used a transfer matrix approach to study the thermo-electro-mechanical characteristics of laminated plates. Dube et al. [18] have presented an exact solution for a simply supported single-layer piezothermoelastic plate with its edges grounded.

An asymptotic theory of leading-order approximation for thin homogeneous single-layer piezoelectric plates has been proposed [19, 20]. The three-dimensional electroelastic analysis has also been conducted for laminated plates [21, 22] using asymptotic theories of higher order approximations. It has been found that solutions of the three-dimensional electroelasticity equations, excluding boundary layer effects, can be generated by successively solving two-dimensional plate equations

Received 21 December 1998; accepted 4 April 1999.

This work was partially supported by the ARO grant DAAG55-98-1-0030 and the NSF grant CMS9713453 to Virginia Polytechnic Institute and State University.

Address correspondence to R. C. Batra, Department of Engineering Science and Mechanics, Mail Code 0219, Virginia Polytechnic Institute and State University, Blacksburg, VA 24061.

from leading order to any higher order. However, none of these electroelasticity approaches considers the thermal effects.

Since the mechanical displacements, transverse stresses, electric potential, and the transverse electric displacement are usually continuous across interlaminar interfaces, they are chosen as the termination parameters in the conventional transfer matrix description for a multilayered stack. Furthermore, employing the asymptotic expansion technique [23, 24] for elastic plates, the conventional transfer matrix method can be refined to enlarge its applications [21, 22]. Here, we combine the asymptotic expansion technique and the transfer matrix formulation to analyze three-dimensional deformations of a piezothermoelastic plate. The temperature field is found separately by solving the heat conduction problem. The technique is illustrated by analyzing the deformations of a rectangular piezothermoelastic laminated plate with its edges simply supported and grounded. Numerical results are presented for the plate subjected to thermal loads on its top and bottom surfaces.

FORMULATION OF THE PROBLEM

We use a rectangular Cartesian coordinate system $\{x_i\}$ $(i = 1, 2, 3)$ such that the lower and upper surfaces of the undeformed plate of uniform thickness h lie in the planes $x_3 = 0, h$, where $x_3 = 0$ is the reference plane. Hereafter, a comma followed by a subscript i denotes the partial derivative with respect to x_i and a repeated index implies summation over the range of the index with Latin indices taking values from 1 to 3 and Greek indices from 1 to 2.

For a quasi-static piezothermoelastic problem, the heat conduction equation is uncoupled from the other equations. Thus the temperature field in the plate is assumed to be known a priori. Details for solving the three-dimensional thermal problem are given in the appendix. We denote by τ and $\mathbf{S}$ (components τ_{ij} and S_{ij}) the symmetric stress and strain tensors; by $\mathbf{D}$ and $\mathbf{E}$ (components D_i and E_i) the electric displacement and the electric field vectors; and by $\mathbf{u}$ (component u_i), φ, and T the mechanical displacement vector, the electric potential, and the temperature increment, respectively. Equations governing the quasi-static deformations of a piezothermoelastic body can be grouped into the following three sets [25–27]:

Divergence equations:

$$\nabla^{\mathrm{T}} \cdot \tau = \mathbf{0} \qquad \nabla \cdot \mathbf{D} = 0 \tag{1}$$

Constitutive relations:

$$\tau = \mathbf{c} : \mathbf{S} - \mathbf{e}^{\mathrm{T}} \cdot \mathbf{E} - \lambda T \qquad \mathbf{D} = \mathbf{e} : \mathbf{S} + \boldsymbol{\epsilon} \cdot \mathbf{E} + \mathbf{p} T \tag{2}$$

Gradient equations:

$$\mathbf{S} = \tfrac{1}{2}[\nabla \mathbf{u} + (\nabla \mathbf{u})^{\mathrm{T}}] \qquad \mathbf{E} = -\nabla \varphi \tag{3}$$

The divergence equations (1), with zero body force, electric charge density, and source of internal energy, and the quasi-static approximation $\nabla \times \mathbf{E} = \mathbf{0}$, where ∇ is the three-dimensional gradient operator, express, respectively, the balance of linear momentum and the Gaussian equation of electrostatics. The elastic moduli $\mathbf{c}$, piezoelectric moduli $\mathbf{e}$, dielectric moduli $\boldsymbol{\epsilon}$, stress-temperature coefficients $\boldsymbol{\lambda}$, and pyroelectric coefficients $\mathbf{p}$ are, respectively, fourth-order, third-order, second-order, and first-order tensors for characterizing a piezothermoelastic medium. The components of these tensors exhibit the following symmetries:

$$c_{ijkl} = c_{jikl} = c_{klij} \qquad e_{kij} = e_{kji} \qquad \varepsilon_{ik} = \varepsilon_{ki} \qquad \lambda_{ik} = \lambda_{ki} \tag{4}$$

For a laminated plate comprised of different homogeneous laminae, the material moduli are piecewise constant functions of x_3.

For monoclinic piezothermoelastic materials with reflectional symmetry in $x_3 = \text{const}$ planes, the constitutive relations can be written as

$$\begin{aligned}
\tau_{\alpha\beta} &= c_{\alpha\beta\omega\rho} S_{\omega\rho} + c_{\alpha\beta 33} S_{33} - e_{3\alpha\beta} E_3 - \lambda_{\alpha\beta} T \\
\tau_{\alpha 3} &= 2 c_{\alpha 3 \omega 3} S_{\omega 3} - e_{\omega\alpha 3} E_\omega \\
\tau_{33} &= c_{33\omega\rho} S_{\omega\rho} + c_{3333} S_{33} - e_{333} E_3 - \lambda_{33} T \\
D_\alpha &= 2 e_{\alpha\omega 3} S_{\omega 3} + \varepsilon_{\alpha\omega} E_\omega \\
D_3 &= e_{3\omega\rho} S_{\omega\rho} + e_{333} S_{33} + \varepsilon_{33} E_3 + p_3 T
\end{aligned} \tag{5}$$

These relations, when combined with Eqs. (1) and (3), yield the state-space equation

$$\partial_z \begin{bmatrix} \mathbf{F} \\ \mathbf{G} \end{bmatrix} = \varepsilon \begin{bmatrix} \mathbf{0} & \mathbf{A} \\ \mathbf{B} & \mathbf{0} \end{bmatrix} \begin{bmatrix} \mathbf{F} \\ \mathbf{G} \end{bmatrix} + \varepsilon^2 \begin{bmatrix} \mathbf{0} \\ \mathbf{C} \end{bmatrix} \theta \tag{6}$$

where we have set $T = \varepsilon\theta$, $x_3 = \varepsilon z$, $\partial_z \equiv \partial/\partial z$, $\varepsilon = h/a$, a is a typical in-plane dimension,

$$\mathbf{F} = \begin{bmatrix} u_1 \\ u_2 \\ \tau_{33} \\ D_3 \end{bmatrix} \quad \text{and} \quad \mathbf{G} = \begin{bmatrix} \tau_{13} \\ \tau_{23} \\ u_3 \\ \varphi \end{bmatrix} \tag{7}$$

The 4×4 matrix operators $\mathbf{A}$ and $\mathbf{B}$ and the 4×1 matrix operator $\mathbf{C}$ contain the in-plane differential operator $\partial_\alpha \equiv \partial/\partial x_\alpha$ and depend on z only through the

material moduli. We partition both **A** and **B** into four 2×2 submatrix operators as

$$\mathbf{A}=\begin{bmatrix} \mathbf{I} & -\mathbf{J}_\beta \partial_\beta \\ -\mathbf{J}_\beta^{\mathrm{T}} \partial_\beta & \mathbf{K}_{\beta\rho} \partial_\beta \partial_\rho \end{bmatrix} \qquad \mathbf{B}=\begin{bmatrix} -\mathbf{L}_{\beta\rho} \partial_\beta \partial_\rho & -\mathbf{M}_\beta \partial_\beta \\ -\mathbf{M}_\beta^{\mathrm{T}} \partial_\beta & \mathbf{N} \end{bmatrix} \tag{8}$$

where matrices **I** and **N** are defined by

$$\mathbf{I}=(I^{\omega\alpha})=\begin{bmatrix} c_{1313} & c_{1323} \\ c_{1323} & c_{2323} \end{bmatrix}^{-1} \qquad \mathbf{N}=(N^{\alpha\omega})=\begin{bmatrix} c_{3333} & e_{333} \\ e_{333} & -\varepsilon_{33} \end{bmatrix}^{-1} \tag{9}$$

We have used superscripts, to which the conventional summation also applies, to denote the row and column indices of a matrix element. $\mathbf{J}_\beta$ and $\mathbf{M}_\beta$ are matrices, and each of their elements is a vector defined by

$$\begin{aligned} \begin{bmatrix} J_\beta^{\omega 1} & J_\beta^{\omega 2} \end{bmatrix} &= \begin{bmatrix} \delta_{\omega\beta} & I^{\omega\alpha} e_{\beta\alpha 3} \end{bmatrix} \\ \begin{bmatrix} M_\beta^{\alpha 1} & M_\beta^{\alpha 2} \end{bmatrix} &= \begin{bmatrix} c_{\alpha\beta 33} & e_{3\alpha\beta} \end{bmatrix} \mathbf{N} \end{aligned} \tag{10}$$

and $\mathbf{K}_{\beta\rho}$ and $\mathbf{L}_{\beta\rho}$ are matrices with each of their elements being a tensor defined by

$$\begin{aligned} K_{\beta\rho}^{11} = K_{\beta\rho}^{12} = K_{\beta\rho}^{21} = 0 \qquad K_{\beta\rho}^{22} &= J_\beta^{\omega 2} e_{\rho\omega 3} + \varepsilon_{\beta\rho} \\ L_{\beta\rho}^{\alpha\omega} &= c_{\alpha\beta\omega\rho} - M_\beta^{\alpha 1} c_{33\omega\rho} - M_\beta^{\alpha 2} e_{3\omega\rho} \end{aligned} \tag{11}$$

Here $\delta_{\omega\beta}$ is the Kronecker delta. The subscripts of the corresponding matrix element imply the usual components of a tensor. These submatrices are only related to the material moduli and depend on x_3. The elements of the 4×1 matrix operator **C** are defined by

$$\begin{aligned} \begin{bmatrix} C_3 \\ C_4 \end{bmatrix} &= \mathbf{N} \begin{bmatrix} \lambda_{33} \\ -p_3 \end{bmatrix} \\ C_\alpha = \gamma_{\alpha\beta} \partial_\beta &\equiv (\lambda_{\alpha\beta} - C_3 c_{\alpha\beta 33} - C_4 e_{3\alpha\beta}) \partial_\beta \end{aligned} \tag{12}$$

The in-plane stresses and in-plane electric displacements, which may be discontinuous in x_3, are given by

$$\begin{aligned} \tau_{\alpha\beta} &= L_{\beta\rho}^{\alpha\omega} \partial_\rho u_\omega + M_\beta^{\alpha 1} \tau_{33} + M_\beta^{\alpha 2} D_3 - \gamma_{\alpha\beta} T \\ D_\rho &= J_\rho^{\alpha 2} \tau_{\alpha 3} - K_{\beta\rho}^{22} \partial_\beta \varphi \end{aligned} \tag{13}$$

AN ASYMPTOTIC SCHEME

The general problem of piezothermoelasticity is to determine the fields of mechanical displacement, stress, electric potential, electric displacement, and temperature under applied mechanical, electrical, and thermal loads. The thermal problem is solved in the appendix, and the temperature field is assumed to be known for the following discussion. The mechanical loading is specified by the shear tractions $q_\alpha^\pm$ and the normal pressures $q_3^\pm$ on the plate surfaces, while the electric loading is specified by the applied electric potentials $V^\pm$. Perfect bonding is assumed between the adjoining laminae in the sense that mechanical displacements, surface tractions, temperature, the normal component of the heat flux, electric potential, and the normal component of the electrical displacement are continuous across the interface.

For general mechanical loading conditions (in particular, unequal tractions on the top and bottom surfaces), the transverse shear stresses are of the order $O(\varepsilon^2)$ and the transverse normal stress is of the order $O(\varepsilon^3)$, as in the case of pure elasticity [23]. Accordingly, the surface forcing functions are scaled as

$$\tau_{\alpha 3}(x_\rho, 0) = \varepsilon^2 q_\alpha^-(x_\rho) \qquad \tau_{\alpha 3}(x_\rho, a) = \varepsilon^2 q_\alpha^+(x_\rho) \tag{14}$$

$$\tau_{33}(x_\rho, 0) = -\varepsilon^3 q_3^-(x_\rho) \qquad \tau_{33}(x_\rho, a) = -\varepsilon^3 q_3^+(x_\rho) \tag{15}$$

The surface electric potentials are constructed to be $O(\varepsilon^2)$ [22], that is,

$$\varphi(x_\rho, 0) = \varepsilon^2 V^-(x_\rho) \qquad \varphi(x_\rho, a) = \varepsilon^2 V^+(x_\rho) \tag{16}$$

To find solutions of successive approximations, we expand the field functions **F** and **G** in terms of the small parameter ε as

$$\begin{bmatrix} \mathbf{F} \\ \mathbf{G} \end{bmatrix} = \sum_{n=0}^{\infty} \varepsilon^{2n} \begin{bmatrix} \varepsilon \mathbf{f}^{(n)} \\ \mathbf{g}^{(n)} \end{bmatrix} \tag{17}$$

Then the surface traction conditions (14), (15) and the surface electric potential conditions (16) may be expressed in terms of the components of the expansion terms of **F** and **G**. For the leading order, we have

$$\begin{aligned} &g_\alpha^{(0)}(0) = \tau_{\alpha 3}^{(0)}(0) = 0 \qquad && g_\alpha^{(0)}(a) = \tau_{\alpha 3}^{(0)}(a) = 0 \\ &f_3^{(0)}(0) = \tau_{33}^{(0)}(0) = 0 \qquad && f_3^{(0)}(a) = \tau_{33}^{(0)}(a) = 0 \\ &g_4^{(0)}(0) = \varphi^{(0)}(0) = 0 \qquad && g_4^{(0)}(a) = \varphi^{(0)}(a) = 0 \end{aligned} \tag{18}$$

and, for the remaining orders with $n \geq 0$,

$$\begin{aligned} &g_\alpha^{(n+1)}(0) = \tau_{\alpha 3}^{(n+1)}(0) = q_\alpha^- \delta_{n0} \qquad && g_\alpha^{(n+1)}(a) = \tau_{\alpha 3}^{(n+1)}(a) = q_\alpha^+ \delta_{n0} \\ &f_3^{(n+1)}(0) = \tau_{33}^{(n+1)}(0) = -q_3^- \delta_{n0} \qquad && f_3^{(n+1)}(a) = \tau_{33}^{(n+1)}(a) = -q_3^+ \delta_{n0} \\ &g_4^{(n+1)}(0) = \varphi^{(n+1)}(0) = V^- \delta_{n0} \qquad && g_4^{(n+1)}(a) = \varphi^{(n+1)}(a) = V^+ \delta_{n0} \end{aligned} \tag{19}$$

Substituting expansion (17) into Eq. (6) leads to the recurrence relations

$$\partial_z \mathbf{g}^{(0)} = \mathbf{0} \qquad \partial_z \mathbf{f}^{(n)} = \mathbf{A}\mathbf{g}^{(n)}$$
$$\partial_z \mathbf{g}^{(n+1)} = \mathbf{B}\mathbf{f}^{(n)} + \delta_{n0}\mathbf{C}\theta \qquad (n \geq 0) \tag{20}$$

Integrating these differential equations with respect to z and using the conditions (18) and (19) for the bottom surface, we obtain for $n \geq 0$

$$\mathbf{g}^{(0)} = \begin{bmatrix} 0 \\ 0 \\ U_3^{(0)} \\ 0 \end{bmatrix} \qquad \mathbf{f}^{(n)} = \begin{bmatrix} U_1^{(n)} \\ U_2^{(n)} \\ -q_3^- \delta_{n1} \\ D_0^{(n)} \end{bmatrix} + Q\mathbf{A}\mathbf{g}^{(n)}$$
$$\mathbf{g}^{(n+1)} = \begin{bmatrix} q_1^- \delta_{n0} \\ q_2^- \delta_{n0} \\ U_3^{(n+1)} \\ V^- \delta_{n0} \end{bmatrix} + Q\mathbf{B}\mathbf{f}^{(n)} + \delta_{n0} Q\mathbf{C}\theta \tag{21}$$

where

$$Q(\cdots) \equiv \int_0^z (\cdots)\, dz \tag{22}$$

The basic unknowns are the three components of mechanical displacements and the normal electric displacement at the reference surface $z = 0$ of the plate:

$$U_\omega^{(n)} \equiv u_\omega^{(n)}(x_\rho, 0) \qquad U_3^{(n)} \equiv u_3^{(n)}(x_\rho, 0) \qquad D_0^{(n)} \equiv D_3^{(n)}(x_\rho, 0^+) \tag{23}$$

These unknowns are determined so that conditions (18) and (19) for the tractions and the electric potential on the top surface $z = a$ are satisfied through expressions (21).

According to Eqs. (21), $\mathbf{f}^{(n)}$ can be written as

$$\mathbf{f}^{(n)} = \mathbf{X}^{(n)} + \mathbf{H}^{(n)} \tag{24}$$

where

$$\mathbf{X}^{(n)} = \begin{bmatrix} U_1^{(n)} - z\partial_1 U_3^{(n)} \\ U_2^{(n)} - z\partial_2 U_3^{(n)} \\ 0 \\ D_0^{(n)} \end{bmatrix}$$
$$\mathbf{H}^{(n+1)} = \delta_{n0}\left\{ Q\mathbf{A}\left[\begin{matrix} q_1^- \\ q_2^- \\ 0 \\ V^- \end{matrix} \right] - \left[\begin{matrix} 0 \\ 0 \\ q_3^- \\ 0 \end{matrix} \right] + Q\mathbf{A}\,Q\mathbf{C}\theta \right\} + Q\mathbf{A}\,Q\mathbf{B}(\mathbf{X}^{(n)} + \mathbf{H}^{(n)}) \tag{25}$$

with the leading order $\mathbf{H}^{(0)}$ of the auxiliary function $\mathbf{H}$ being $\mathbf{0}$. Using the notation

$$\overline{Q}(\cdots) \equiv \int_0^a (\cdots)\, dz \tag{26}$$

the traction and the electric potential conditions (19) on the top surface of the plate can be rewritten through Eqs. (21) as

$$\begin{aligned}
\overline{Q} B_{\alpha L} f_L^{(n)} &= \left(q_\alpha^+ - q_\alpha^- - \overline{Q} C_\alpha \theta\right)\delta_{n0} \\
\overline{Q} A_{3L} g_L^{(n+1)} &= -\left(q_3^+ - q_3^-\right)\delta_{n0} \\
\overline{Q} B_{4L} f_L^{(n)} &= \left(V^+ - V^- - \overline{Q} C_4 \theta\right)\delta_{n0}
\end{aligned} \tag{27}$$

where the subscript L takes values from 1 to 4 and the summation convention also applies to L. Furthermore, using Eqs. (21) and (24) and noting that $A_{3\alpha} = -\partial_\alpha$ and $A_{33} = A_{34} = 0$, Eqs. (27) can be rewritten as

$$\tilde{\mathbf{R}}\tilde{\mathbf{X}}^{(n)} (\equiv \mathbf{R}\mathbf{X}^{(n)}) = \delta_{n0}\mathbf{Y} - \mathbf{R}\mathbf{H}^{(n)} \tag{28}$$

where

$$\tilde{\mathbf{X}}^{(n)} = \left[U_1^{(n)} \quad U_2^{(n)} \quad U_3^{(n)} \quad D_0^{(n)}\right]^{\mathrm{T}} \tag{29}$$

The components of the matrix operators $\tilde{\mathbf{R}}$ and $\mathbf{R}$ are

$$\begin{aligned}
&\tilde{R}_{\alpha\omega} = R_{\alpha\omega} = -\overline{Q} L_{\beta\rho}^{\alpha\omega} \partial_\beta \partial_\rho \qquad \tilde{R}_{\alpha 3} = \overline{Q}_z L_{\beta\rho}^{\alpha\omega} \partial_\beta \partial_\omega \partial_\rho \qquad R_{\alpha 3} = -\overline{Q} M_\beta^{\alpha 1} \partial_\beta \\
&\tilde{R}_{\alpha 4} = R_{\alpha 4} = -\overline{Q} M_\beta^{\alpha 2} \partial_\beta \qquad \tilde{R}_{3\omega} = R_{3\omega} = -\overline{Q} z L_{\beta\rho}^{\alpha\omega} \partial_\alpha \partial_\beta \partial_\rho \\
&\tilde{R}_{33} = \overline{Q} z^2 L_{\beta\rho}^{\alpha\omega} \partial_\alpha \partial_\beta \partial_\omega \partial_\rho \qquad R_{33} = -\overline{Q} z M_\beta^{\alpha 1} \partial_\alpha \partial_\beta \\
&\tilde{R}_{34} = R_{34} = -\overline{Q} z M_\beta^{\alpha 2} \partial_\alpha \partial_\beta \qquad \tilde{R}_{4\omega} = R_{4\omega} = -\overline{Q} M_\beta^{\omega 2} \partial_\beta \\
&\tilde{R}_{43} = \overline{Q} z M_\beta^{\omega 2} \partial_\beta \partial_\omega \qquad R_{43} = \overline{Q} N^{21} \qquad \tilde{R}_{44} = R_{44} = \overline{Q} N^{22}
\end{aligned} \tag{30}$$

and the components of $\mathbf{Y}$ involved in the effective loads on the right-hand side of Eq. (28) are

$$\begin{aligned}
Y_\alpha &= q_\alpha^+ - q_\alpha^- - \overline{Q}\gamma_{\alpha\beta}\partial_\beta\theta \\
Y_3 &= -\left(q_3^+ - q_3^-\right) + a\partial_\alpha q_\alpha^+ - \overline{Q} z \gamma_{\alpha\beta}\partial_\alpha\partial_\beta\theta \\
Y_4 &= V^+ - V^- - \overline{Q} C_4 \theta
\end{aligned} \tag{31}$$

Equations (28) are the key field equations obtained through the asymptotic approach from which the unknowns (29) of each order can be solved with specified edge conditions on the reference plane. Since $\mathbf{H}^{(0)} = \mathbf{0}$ and $\mathbf{Y}$ is known a priori from Eq. (31), the unknowns of the leading order can be determined from the field equation of the leading order. Then $\mathbf{H}^{(1)}$ can be obtained from Eq. (25). Such a procedure may be continued to solve for higher order unknowns. Since the matrix operators $\tilde{\mathbf{R}}$ and $\mathbf{R}$ appearing in Eq. (28) have the same form for the field equations of all orders, a full three-dimensional solution in the interior of the plate can easily be obtained. In particular, the differential operator $\tilde{\mathbf{R}}$ is a generalization of that for the bending of classical monoclinic laminated elastic plates [28].

EXAMPLES

For the linear problems being studied herein, the deformations due to mechanical, electrical, and thermal loads can be studied separately and then superposed to ascertain deformations due to the combined loads. Cheng et al. [22] have analyzed the deformations of a piezoelectric plate due to mechanical and electrical loads; accordingly we consider only thermal loads.

We analyze here thermo-electro-mechanical deformations of a simply supported rectangular plate subjected to the following thermal boundary conditions on the top and bottom surfaces and edges:

$$-T_{,3} + h_1 T = h_1 T^{-} \quad \text{at } x_3 = 0 \qquad T_{,3} + h_2 T = h_2 T^{+} \quad \text{at } x_3 = h \tag{32}$$

$$T = 0 \quad \text{at } x_1 = 0, a \qquad T = 0 \quad \text{at } x_2 = 0, b \tag{33}$$

$$T^{\pm} = \hat{T}^{\pm} \sin \frac{\pi}{a} x_1 \sin \frac{\pi}{b} x_2 \tag{34}$$

where h_1 and h_2 are, respectively, the heat transfer coefficients at the bottom and top surfaces. The mechanical and electrical boundary conditions on the top and bottom surfaces, and at the edges $x_1 = 0, a$ and $x_2 = 0, b$ are

$$\begin{aligned} &q_\alpha^{\pm} = 0, q_3^{\pm} = 0, V^{\pm} = 0 \quad \text{at } x_3 = 0, h \\ &u_2 = u_3 = \tau_{11} = \varphi = 0 \quad \text{at } x_1 = 0, a \\ &u_1 = u_3 = \tau_{22} = \varphi = 0 \quad \text{at } x_2 = 0, b \end{aligned} \tag{35}$$

That is, the edges besides being simply supported are grounded, and the top and bottom surfaces are grounded and free of surface tractions. Guided by the form

(34) of $T^{\pm}$ and the boundary conditions (35), we assume that

$$\tilde{\mathbf{X}}^{(n)} = \begin{bmatrix} U_1^{(n)} \\ U_2^{(n)} \\ U_3^{(n)} \\ D_0^{(n)} \end{bmatrix} = \begin{bmatrix} \hat{U}_1^{(n)} \cos \dfrac{\pi}{a} x_1 \sin \dfrac{\pi}{b} x_2 \\ \hat{U}_2^{(n)} \sin \dfrac{\pi}{a} x_1 \cos \dfrac{\pi}{b} x_2 \\ \hat{U}_3^{(n)} \sin \dfrac{\pi}{a} x_1 \sin \dfrac{\pi}{b} x_2 \\ \hat{D}_0^{(n)} \sin \dfrac{\pi}{a} x_1 \sin \dfrac{\pi}{b} x_2 \end{bmatrix} \tag{36}$$

where a quantity with a superimposed hat denotes a constant. Edge conditions in Eq. (35) are identically satisfied by Eq. (36), and there are no boundary layer effects for this problem. Therefore, a three-dimensional piezothermoelasticity solution may be generated to any desired degree of numerical accuracy.

The physical quantities are nondimensionalized by

$$\bar{u}_i = \frac{u_i}{Pa} \qquad \bar{\tau}_{ij} = \frac{\tau_{ij}}{Pc^*} \qquad \bar{\varphi} = \frac{e^* \varphi}{Pac^*}$$
$$\bar{D}_i = \frac{D_i}{Pe^*} \qquad \bar{T} = \frac{\alpha^* T}{P} \qquad \bar{E}_i = \frac{e^* E_i}{Pc^*} \tag{37}$$

where $P = \alpha^* T^+$. Values of nonvanishing material moduli of *cadmium selenide crystal* (CSC) [18] and the *fiber-reinforced composite* (FRC) [29], the two materials studied herein, are listed in Table 1. Note that the piezoelectric moduli for the FRC vanish but the dielectric moduli are nonzero.

Computed results for a single-layer (CSC) plate with the aspect ratio $a/b = 0\,(b \to \infty)$; the span-to-thickness ratio $a/h = 2, 10$; $T^- = 0$; the heat transfer coefficients $h_1 = 0.2/h$, $h_2 = 2/h$; and the corresponding values from the exact solution of [18] are given in Table 2. We have set $c^* = 42.785 \times 10^9 \text{Nm}^{-2}$, $e^* = 0.16788$ Cm^{-2}, and $\alpha^* = 4.396 \times 10^{-6}$ K^{-1}. The order of the present solution is increased from 0 to 7 where the higher order solutions are obtained via the recurrence procedure described previously. Numerical convergence to five significant digits is attained for the seventh-order solution, which is in excellent agreement with the exact results of [18], even for the very thick plate ($a/h = 2$). The mechanical displacements and the transverse electric displacement of the leading order are reasonably good, especially for a thin plate; while the out-of-plane stresses of first order are not acceptable. This means that the classical thin-plate theory cannot give good values of the out-of-plane stresses even if they are obtained by a posteriori calculation, which is precisely equivalent to the first-order approximation.

In the second example we present results for a four-ply (CSC/90° FRC/0° FRC/CSC starting from the bottom) laminated plate with each ply having the same thickness. The span-to-thickness ratio, a/h, equals 4 (thick), 10 (moderately thick), or 50 (thin). The plate is infinitely wide ($b \to \infty$), thus we have $u_2 = D_2 =$

Table 1 Values of nonvanishing material moduli

Moduli	CSC	FRC
$c_{1111}(10^9\,\mathrm{N/m^2})$	74.1	173.66
$c_{2222}(10^9\,\mathrm{N/m^2})$	74.1	7.3909
$c_{3333}(10^9\,\mathrm{N/m^2})$	83.6	7.3909
$c_{1122}(10^9\,\mathrm{N/m^2})$	45.2	2.3154
$c_{1133}(10^9\,\mathrm{N/m^2})$	39.3	2.3154
$c_{2233}(10^9\,\mathrm{N/m^2})$	39.3	1.8709
$c_{2323}(10^9\,\mathrm{N/m^2})$	13.17	1.38
$c_{3131}(10^9\,\mathrm{N/m^2})$	13.17	3.45
$c_{1212}(10^9\,\mathrm{N/m^2})$	14.45	3.45
$e_{311}(\mathrm{C/m^2})$	−0.16	0
$e_{322}(\mathrm{C/m^2})$	−0.16	0
$e_{333}(\mathrm{C/m^2})$	0.347	0
$e_{113}(\mathrm{C/m^2})$	−0.138	0
$\varepsilon_{11}(10^{-12}\,\mathrm{F/m})$	82.5	30.95
$\varepsilon_{22}(10^{-12}\,\mathrm{F/m})$	82.5	26.53
$\varepsilon_{33}(10^{-12}\,\mathrm{F/m})$	90.2	26.53
$\lambda_{11}(10^6\,\mathrm{N/m^2K})$	0.621	0.26384
$\lambda_{22}(10^6\,\mathrm{N/m^2K})$	0.621	0.33104
$\lambda_{33}(10^6\,\mathrm{N/m^2K})$	0.551	0.33104
$p_3(10^{-6}\,\mathrm{C/m^2K})$	−2.94	0
$\kappa_{11}(\mathrm{W/mK})$	1	36.42
$\kappa_{22}(\mathrm{W/mK})$	1	0.96
$\kappa_{33}(\mathrm{W/mK})$	1.5	0.96

Table 2 Comparison of the present solution for a single-layer (CSC) plate ($a/b=0$) with the exact results of Dube et al. [18]

Order	0	1	7	Exact [18]
	$a/h=2$			
$\bar{u}_1(0,h)\times 100$	−26.964	−29.650	−29.330	−29.33
$\bar{u}_3(a/2,\,h/2)\times 100\varepsilon$	4.9323	4.8591	4.8325	4.832
$\bar{\tau}_{11}(a/2,\,h)\times 100/\varepsilon^2$	−45.135	−0.9015	−6.2360	−6.236
$\bar{\tau}_{13}(0,\,h/4)\times 100/\varepsilon^3$	0	11.951	1.6600	1.660
$\bar{\tau}_{33}(a/2,\,h/2)\times 100/\varepsilon^4$	0	12.668	1.7589	1.759
$\bar{\varphi}(a/2,\,h/2)\times 10000/\varepsilon$	0	11.086	8.9460	8.946
$\bar{D}_3(a/2,0)$	−1.5228	−1.3895	−1.4312	−1.431
	$a/h=10$			
$\bar{u}_1(0,\,h)\times 100$	−42.109	−42.286	−42.285	−42.28
$\bar{u}_3(a/2,\,h/2)\times 100\varepsilon$	2.5019	2.5001	2.5001	2.500
$\bar{\tau}_{11}(a/2,\,h)\times 100/\varepsilon^2$	−86.662	−13.445	−13.860	−13.86
$\bar{\tau}_{13}(0,\,h/4)\times 100/\varepsilon^3$	0	24.914	4.0641	4.064
$\bar{\tau}_{33}(a/2,\,h/2)\times 100/\varepsilon^4$	0	26.161	4.2580	4.258
$\bar{\varphi}(a/2,\,h/2)\times 10000/\varepsilon$	0	5.6321	5.5794	5.579
$\bar{D}_3(a/2,0)$	−3.0255	−3.0231	−3.0231	−3.023

Table 3 Present results for a four-ply (CSC / 90°FRC / 0°FRC / CSC) laminate ($a/b = 0$)

	$a/h = 4$	$a/h = 10$	$a/h = 50$
$\overline{u}_1(0, 0)$	−0.1911	−0.9384	−1.488
$\overline{u}_3(a/2, 0)$	0.3965	−1.182	−13.60
$\overline{u}_3(a/2, h)$	1.584	0.1616	−13.21
$\overline{\tau}_{11}(a/2, h)$	−68.58	−154.4	−216.9
$\overline{\tau}_{22}(a/2, h)$	−133.6	−216.2	−275.0
$\overline{\tau}_{13}(0, 3h/4)$	−11.15	−10.59	−3.000
$\overline{\tau}_{33}(a/2, 3h/4)$	1.166	0.4357	0.02463
$\overline{\varphi}(a/2, h/2)$	0.1721	−0.01039	−0.01486
$\overline{D}_1(0, (h/2)^+)$	−0.01673	0.001011	0.001445
$\overline{D}_3(a/2, 0)$	−0.1301	−0.2683	−0.3622
$\overline{T}(a/2, 0)$	0.1343	0.4727	0.7219
$\overline{T}(a/2, h)$	0.5445	0.7644	0.9169

$\tau_{12} = \tau_{23} = 0$. All the loading conditions and boundary conditions are the same as in the first example. The converged values of the dimensionless variables defined by Eq. (39) with $c^* = 10^9 \text{Nm}^{-2}$, $e^* = 1\ \text{Cm}^{-2}$, and $\alpha^* = 10^{-6}\text{K}^{-1}$ and accurate to four significant digits are given in Table 3. For the thick laminate, the converged solution is fourteenth order, and it is of lower order for the other two laminates. Since transverse deflections of corresponding points on the top and bottom surfaces are quite different especially for thick or moderately thick plates, the assumption of a constant through-the-thickness deflection made in most two-dimensional plate theories is not good.

For the plate considered in the second example with $a/h = 10$, Figures 1(a–c) depict, respectively, the through-thickness variations of the transverse shear stress on the section $x_1 = 0$, the transverse normal stress on the plane $x_1 = a/2$, and the longitudinal stress on the plane $x_1 = a/2$. The transverse shear and transverse normal stresses are negligible as compared to the longitudinal stress. The longitudinal stress is compressive and varies affinely in the two CSC layers and the lower 90° FRC layer; it is tensile and varies nonaffinely in the 0° FRC layer. Figures 2(a–c) exhibit, respectively, the through-thickness distributions of the electric potential on the section $x_1 = a/2$, electric field E_1 on the section $x_1 = 0$, and the electric field E_3 on the plane $x_1 = a/2$. All three fields vary affinely through each layer, and the transverse electric field is constant in the two FRC layers.

CONCLUSIONS

We used an asymptotic expansion technique combined with the transfer matrix method to delineate three-dimensional deformations of a linear piezothermoelastic laminate subjected to mechanical, electrical, and thermal loads on its top and bottom surfaces. We computed numerical results for a single-layer plate and a four-layer laminate made of CSC, 90° FRC, 0° FRC, and CSC with the top and

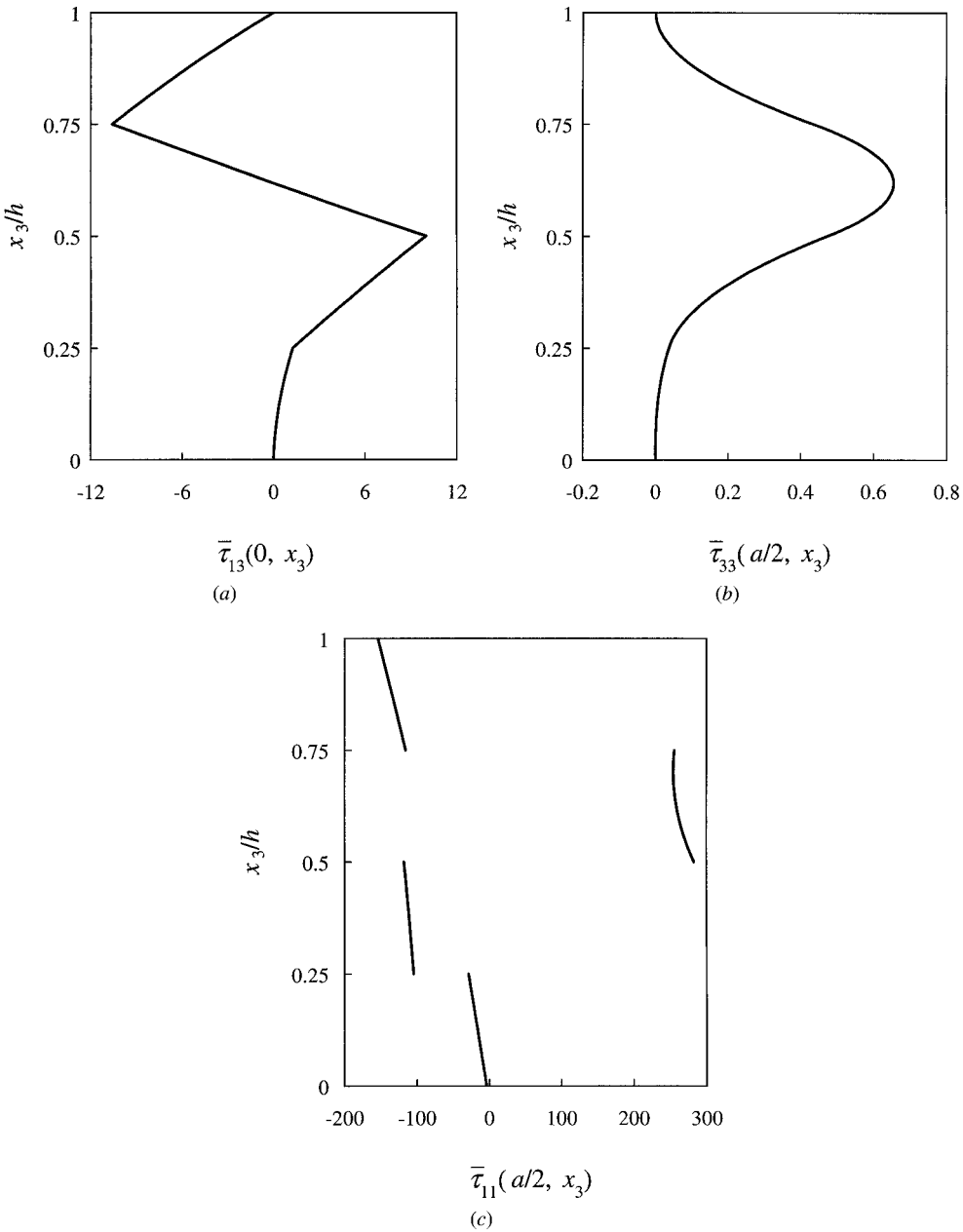

Figure 1. The through-thickness variation of (*a*) the transverse shear stress on the plane $x_1 = 0$, (*b*) the transverse normal stress on the section $x_1 = a/2$, and (*c*) the longitudinal stress on the plane $x_1 = a/2$.

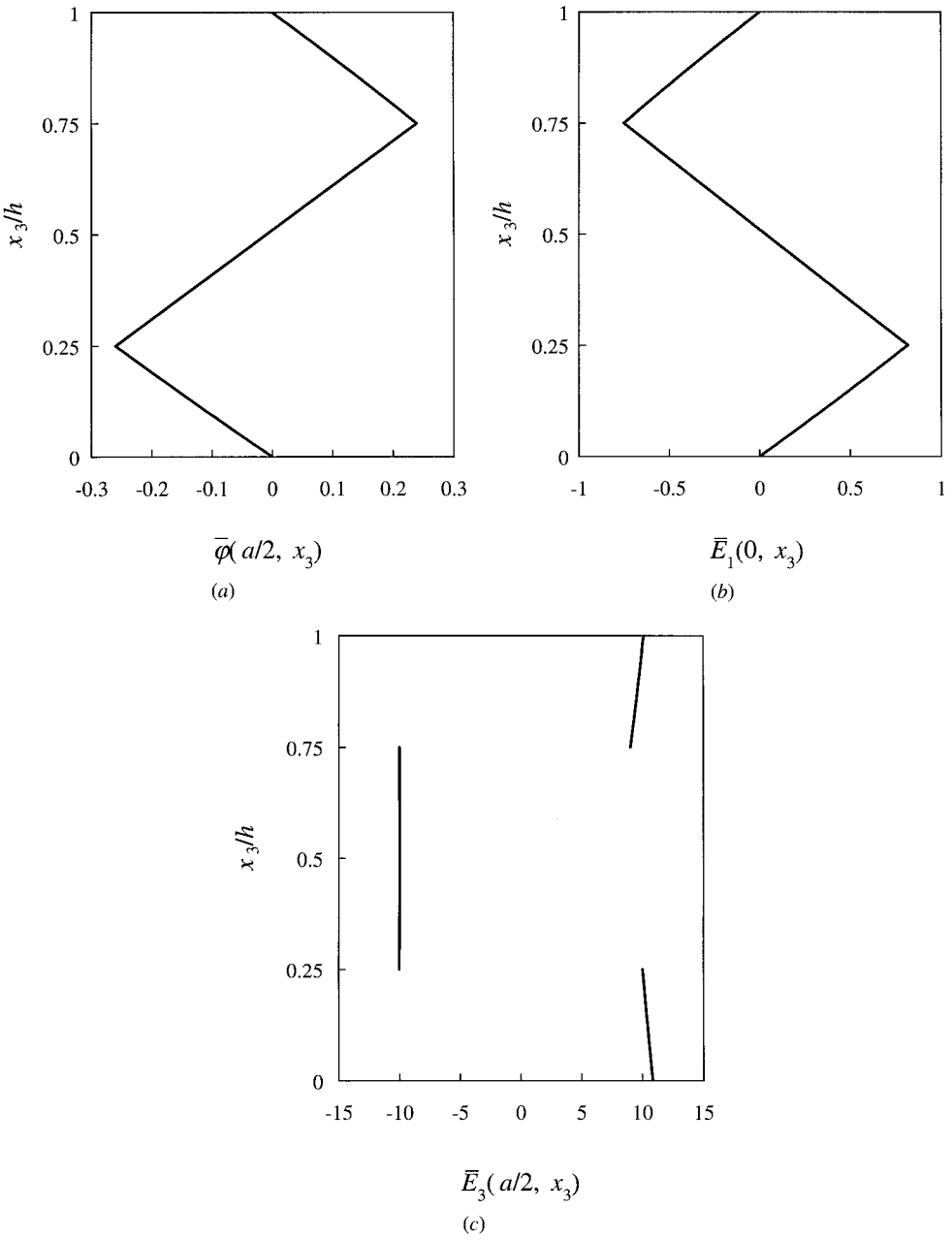

Figure 2. The through-thickness distribution of (*a*) the electric potential on the plane $x_1 = a/2$, (*b*) the electric field E_1 on the section $x_1 = 0$, and (*c*) the electric field E_3 on the plane $x_1 = a/2$.

bottom surfaces electrically grounded and subjected only to thermal loads. It was found that the solution converges rather rapidly even for very thick laminates. Computed results for a simply supported rectangular plate with its edges grounded are found to closely match those from the analytical solution of the problem. The transverse deflections of corresponding points on the top and bottom surfaces differ significantly, thereby implying noticeable changes in the plate thickness.

REFERENCES

1. E. F. Crawley and J. de Luis, Use of Piezoelectric Actuators as Elements of Intelligent Structures, *AIAA J.*, vol. 25, pp. 1373–1385, 1987.
2. H. S. Tzou, *Piezoelectric Shells*: *Distributed Sensing and Control of Continua*, Kluwer Academic Publishers, Dordrecht, 1993.
3. Y. S. Zhou and H. F. Tiersten, Elastic Analysis of Laminated Composite Plates in Cylindrical Bending due to Piezoelectric Actuators, *Smart Mater. Struct.*, vol. 3, pp. 255–265, 1994.
4. R. C. Batra, X. Q. Liang, and J. S. Yang, Shape Control of Vibrating Simply Supported Rectangular Plates, *AIAA J.*, vol. 34, pp. 116–122, 1996.
5. R. C. Batra, X. Q. Liang, and J. S. Yang, The Vibration of a Simply Supported Rectangular Elastic Plate due to Piezoelectric Actuators, *Int. J. Solids Struct.*, vol. 33, pp. 1597–1618, 1996.
6. R. C. Batra, and X. Q. Liang, The Vibration of a Rectangular Laminated Elastic Plate with Embedded Piezoelectric Sensors and Actuators, *Comput. Struct.*, vol. 63, pp. 203–216, 1997.
7. J. N. Reddy, On Laminated Composite Plates with Integrated Sensors and Actuators, *Engrg. Struct.*, 1999 (in press).
8. T. R. Tauchert, Piezothermoelastic Behavior of a Laminated Plate, *J. Thermal Stresses*, vol. 15, pp. 25–37, 1992.
9. T. R. Tauchert, Cylindrical Bending of Hybrid Laminates under Thermo-Electro-Mechanical Loading, *J. Thermal Stresses*, vol. 19, pp. 287–296, 1996.
10. F. Ashida, T. R. Tauchert, and N. Noda, Response of a Piezothermoelastic Plate of Crystal Class 6mm Subject to Axisymmetric Heating, *Int. J. Engrg. Sci.*, vol. 31, pp. 373–384, 1993.
11. F. Ashida, T. R. Tauchert, and N. Noda, Potential Function Method for Piezothermoelastic Problems of Solids of Crystal Class 6mm in Cylindrical Coordinates, *J. Thermal Stresses*, vol. 17, pp. 361–376, 1994.
12. F. Ashida, T. R. Tauchert, and N. Noda, A General Technique for Piezothermoelasticity of Hexagonal Solids of Class 6mm in Cartesian Coordinates, *ZAMM*, vol. 74, pp. 87–97, 1994.
13. N. Noda and S. Kimura, Deformation of a Piezothermoelectric Composite Plate Considering the Coupling Effect, *J. Thermal Stresses*, vol. 21, pp. 359–379, 1998.
14. J. S. Yang and R. C. Batra, A Theory of Electroded Thin Thermopiezoelectric Plates Subject to Large Driving Voltages, *J. Appl. Phys.*, vol. 76, pp. 5411–5417, 1994.
15. J. S. Yang and R. C. Batra, Free-Vibrations of a Linear Thermopiezoelectric Body, *J. Thermal Stresses*, vol. 18, pp. 247–262, 1995.
16. K. Xu, A. K. Noor, and Y. Y. Tang, Three-Dimensional Solutions for Coupled Thermo-electroelastic Response of Multilayered Plates, *Comput. Methods Appl. Mech. Engrg.*, vol. 126, pp. 355–371, 1995.
17. K. Xu, A. K. Noor, and Y. Y. Tang, Three-Dimensional Solutions for Free Vibrations of Initially-Stressed Termoelectroelastic Multilayered Plates, *Comput. Methods Appl. Mech. Engrg.*, vol. 141, pp. 125–139, 1997.
18. G. P. Dube, S. Kapuria, and P. C. Dumir, Exact Piezothermoelastic Solution of Simply-Supported Orthotropic Flat Panel in Cylindrical Bending, *Int. J. Mech. Sci.*, vol. 38, pp. 1161–1177, 1996.
19. G. A. Maugin and D. Attou, An Asymptotic Theory of Thin Piezoelectric Plates, *Quart. J. Mech. Appl. Math.*, vol. 43, pp. 347–362, 1990.
20. P. Bisegna and F. Maceri, A Consistent Theory of Thin Piezoelectric Plates, *J. Intell. Mater. Syst. Struct.*, vol. 7, pp. 372–389, 1996.

21. Z. Q. Cheng, C. W. Lim, and S. Kitipornchai, Three-Dimensional Exact Solution for Inhomogeneous and Laminated Piezoelectric Plates, *Int. J. Engrg. Sci.*, 1999 (in press).
22. Z. Q. Cheng, C. W. Lim, and S. Kitipornchai, Three-Dimensional Asymptotic Approach to Inhomogeneous and Laminated Piezoelectric Plates, *Int. J. Solids Struct.*, 1999 (in press).
23. Y. M. Wang and J. Q. Tarn, A Three-Dimensional Analysis of Anisotropic Inhomogeneous and Laminated Plates, *Int. J. Solids Struct.*, vol. 31, pp. 497–515, 1994.
24. J. Q. Tarn and Y. M. Wang, Asymptotic Thermoelastic Analysis of Anisotropic Inhomogeneous and Laminated Plates, *J. Thermal Stresses*, vol. 18, pp. 35–58, 1995.
25. H. F. Tiersten, *Linear Piezoelectric Plate Vibrations*, Plenum Press, New York, 1969.
26. R. D. Mindlin, Equations of High Frequency Vibrations of Thermopiezoelectric Crystal Plates, *Int. J. Solids Struct.*, vol. 10, pp. 625–632, 1974.
27. A. C. Eringen and G. A. Maugin, *Electrodynamics of Continua*, Springer-Verlag, New York, 1990.
28. J. N. Reddy, *Mechanics of Laminated Composite Plates*: *Theory and Analysis*, CRC Press, Boca Raton, FL, 1997.
29. V. B. Tungikar and K. M. Rao, Three-Dimensional Exact Solution of Thermal Stresses in Rectangular Composite Laminate, *Compos. Struct.*, vol. 27, pp. 419–430, 1994.

APPENDIX A. SOLUTION FOR THE HEAT CONDUCTION PROBLEM

We consider a rectangular laminated plate with k plies made of different homogeneous orthotropic materials. The distance of the top surface of the mth ply from the bottom-most surface of the plate is ${}^{(m)}h$, in particular, ${}^{(k)}h = h$. The temperature field at any point of the plate is given by

$$T(x_i) = {}^{(1)}TH(x_3) + \sum_{m=1}^{k-1} ({}^{(m+1)}T - {}^{(m)}T)\, H(x_3 - {}^{(m)}h) \tag{A.1}$$

where $H(x_3)$ is the Heaviside step function. The temperature ${}^{(m)}T$ in the mth ply $(m = 1, \ldots, k)$ satisfies the steady-state heat conduction equation

$${}^{(m)}\kappa_{11}\, {}^{(m)}T_{,11} + {}^{(m)}\kappa_{22}\, {}^{(m)}T_{,22} + {}^{(m)}\kappa_{33}\, {}^{(m)}T_{,33} = 0 \tag{A.2}$$

where ${}^{(m)}\kappa_{11}$, ${}^{(m)}\kappa_{22}$, and ${}^{(m)}\kappa_{33}$ are, respectively, the thermal conductivity coefficients in the x_1-, x_2-, and x_3-directions for the mth ply. For boundary conditions (32) and (33) with $T^{\pm}$ given by Eq. (34), the temperature in the mth ply can be taken as

$${}^{(m)}T = {}^{(m)}\hat{T} \sin\frac{\pi}{a}x_1 \sin\frac{\pi}{b}x_2 \tag{A.3}$$

where

$$\begin{aligned} {}^{(m)}\hat{T} &= \frac{{}^{(m)}\hat{T}^{+}\,\mathrm{sh}^{(m)}\mu(x_3 - {}^{(m-1)}h) - {}^{(m)}\hat{T}^{-}\,\mathrm{sh}^{(m)}\mu(x_3 - {}^{(m)}h)}{\mathrm{sh}^{(m)}\mu({}^{(m)}h - {}^{(m-1)}h)} \\ {}^{(m)}\mu^2 &= \pi^2 \frac{{}^{(m)}\kappa_{11}b^2 + {}^{(m)}\kappa_{22}a^2}{{}^{(m)}\kappa_{33}a^2b^2} \end{aligned} \tag{A.4}$$

sh $x \equiv \text{sinhyp}(x)$, and ${}^{(m)}\hat{T}^{\pm}$ equals the value of ${}^{(m)}\hat{T}$ at the top and bottom surfaces of the mth ply. The temperature field (A.3) identically satisfies Eq. (A.2).

Assuming the condition of ideal thermal contact between adjacent plies, that is,

$$
\begin{aligned}
&{}^{(m+1)}T = {}^{(m)}T \\
&{}^{(m+1)}\kappa_{33}\,{}^{(m+1)}T_{,3} = {}^{(m)}\kappa_{33}\,{}^{(m)}T_{,3} \quad \text{at } x_3 = {}^{(m)}h \,(m = 1, \ldots, k-1)
\end{aligned} \tag{A.5}
$$

we have

$$
\begin{aligned}
&{}^{(m+1)}\hat{T}^{-} = {}^{(m)}\hat{T}^{+} \\
&{}^{(m+1)}\kappa_{33}\,{}^{(m+1)}\mu \frac{{}^{(m+1)}\hat{T}^{+} - {}^{(m+1)}\hat{T}^{-}\,\text{ch}^{(m+1)}\mu({}^{(m+1)}h - {}^{(m)}h)}{\text{sh}^{(m+1)}\mu({}^{(m+1)}h - {}^{(m)}h)} \\
&\quad = {}^{(m)}\kappa_{33}\,{}^{(m)}\mu \frac{{}^{(m)}\hat{T}^{+}\text{ch}^{(m)}\mu({}^{(m)}h - {}^{(m-1)}h) - {}^{(m)}\hat{T}^{-}}{\text{sh}^{(m)}\mu({}^{(m)}h - {}^{(m-1)}h)} \qquad (m = 1, \ldots, k-1)
\end{aligned} \tag{A.6}
$$

where $\text{ch}\, x \equiv \text{coshyp}(x)$. The condition (34) for the bottom-most and top-most surfaces of the plate gives

$$
\begin{aligned}
&-\frac{{}^{(1)}\mu}{h_1 \text{sh}^{(1)}\mu^{(1)}h}\,{}^{(1)}\hat{T}^{+} + \left[1 + \frac{{}^{(1)}\mu\,\text{cth}^{(1)}\mu^{(1)}h}{h_1}\right]{}^{(1)}\hat{T}^{-} = \hat{T}^{-} \\
&\left[1 + \frac{{}^{(k)}\mu\,\text{cth}^{(k)}\mu(h - {}^{(k-1)}h)}{h_2}\right]{}^{(k)}\hat{T}^{+} - \frac{{}^{(k)}\mu}{h_2 \text{sh}^{(k)}\mu(h - {}^{(k-1)}h)}\,{}^{(k)}\hat{T}^{-} = \hat{T}^{+}
\end{aligned} \tag{A.7}
$$

where $\text{cth}\ x \equiv \text{cothyp}(x)$. The $2k$ unknowns ${}^{(m)}\hat{T}^{\pm}$ $(m = 1, \ldots, k)$ can be determined from the $2k$ linear equations (A.6) and (A.7).